

Influence of pH on the Structural and Optical Properties of Polycrystalline MnTe₂ Thin Films Produced by Chemical Bath Deposition Method

İ.A. KARİPER^a AND F. GÖDE^{b,*}

^aErciyes University, Primary Education Department, Kayseri, Turkey
and

Erciyes Teknopark, Kayseri, Turkey

^bMehmet Akif Ersoy University, Physics Department, Burdur, Turkey

Polycrystalline manganese ditelluride (MnTe₂) thin films are synthesized on commercial glass substrates by chemical bath deposition technique at different pH values (pH = 9, 10, 11 and 12). The effect of pH on the structural and optical properties of chemically deposited MnTe₂ thin films have been investigated in this study. The structure and optical properties of the films are characterized by X-ray diffraction and optical absorption spectroscopy. The X-ray diffraction results suggest that the films are polycrystalline with a mixture of dominant cubic MnTe₂ phase and few traces of orthorhombic MnTeO₃ and MnTe₂O₅ phases. The optical band gap of the films increases approximately from 1.66 eV to 2.62 eV with increasing pH. Moreover, optical parameters of the films such as refractive index, extinction coefficient, real and imaginary dielectric constants are investigated using absorption and transmittance spectra taken from the UV-vis spectrophotometer. At 600 nm wavelength, refractive index and extinction coefficient values vary in the range of 1.39–1.55 and 0.17–0.23, respectively. An increase in optical band gap could be attributed to the quantum confinement effect.

DOI: [10.12693/APhysPolA.132.531](https://doi.org/10.12693/APhysPolA.132.531)

PACS/topics: X-ray diffraction, thin film, optical constant, growth from solutions

1. Introduction

In recent years, diluted magnetic semiconductors (DMSs) have attracted much interests because of various phenomena related to antiferromagnetic spin coupling between neighboring magnetic ions, the large *sp-d* interaction between the band electrons and magnetic ions which gives rise to several magneto-optical effects, phase transition, and other effects [1]. Materials containing Cr, Mn, Fe, Co, and Ni called dilute magnetic semiconductor (DMSs) materials [2], combining traditional semiconductors with spin magnetism are promising for semiconductor spintronic applications. These materials are also studied by other researchers. Ünlü [3] investigated weak interaction properties of Fe and Ni isotopes. Ucar et al. [4] reported the microstructure of boride binary (Ni–Ti) and ternary (Ni–Ti–Cu) shape memory alloys. Laslouni et al. [5] studied magnetic properties and resistivity measurement of nanocrystalline Cu₇₀Fe₁₈Co₁₂ alloys. Ustundağ and Aslan [6] investigated electronic and magnetic properties of Ca-doped Mn-ferrite. Boubaker and Said [7] reported the structural, elastic and mechanical properties of Mn₃Sb intermetallic compound by using *ab initio* calculations. Karahan and Tiltel [8] studied corrosive properties of environmental ZnFe/polyaniline on low carbon steel by using electrodeposition technique.

Sahin et al. [9] investigated the influence of Pd addition in CoCrMo alloys produced by investment casting method. Djamal et al. [10] reported development of giant magnetoresistance material based on cobalt ferrite (CoFe₂O₄) prepared by opposed target magnetron sputtering onto silicon substrate. Sylva et al. [11] studied the effect of temperature and time on the growth of the nitrided layer and its characteristics for the gas-nitrided 31CrMoV9 alloy steel. Karip et al. [12] investigated the effect of Fe–Cr and Fe–B with massive wire based hardfacing alloys.

Manganese ditelluride (MnTe₂), a manganese chalcogenide, is a II–VI semiconductor compound and is important for optoelectronic devices, solar cells [13], IR detectors, sensors and lasers applications due to its chemical stability, structural, optical and electrical properties. Most of the studies in the literature is on the structural, optical and electrical properties of manganese monoteleluride (MnTe). It has *p*-type conductivity with a direct narrow band gap (1.3 eV) [14], which is close to optimum for photo-conversion [15] and direct band gap of SnS thin films (1.17–1.40 eV) [16]. Wu et al. [17] showed MnTe polycrystalline samples having *p*-type conductivity. Wang et al. [18] reported effect of adding Cr on magnetic properties and metallic behavior in MnTe film.

But, there is no report on the structural and optical properties of MnTe₂ thin films synthesized by chemical bath deposition (CBD) method using different pH values to date. Out of other thin films production techniques, CBD method is an attracting considerable attention as it does not require sophisticated instrumentation like vacuum system, high temperature system and other

*corresponding author; e-mail: ftmgode@gmail.com

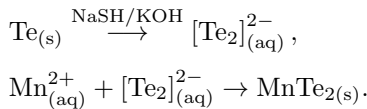
expensive equipments. It is low cost, simple and convenient wet chemical method that has been previously used for deposition of a variety of metal chalcogenide thin films [16, 19, 20]. In CBD method, different substrates such as insulators, semiconductors and metals, and a large number of substrates can be coated in a single run with a proper jig design. Attractive features of this method are the convenience in large area deposition at low evaporation temperature with the possibility to control film thickness and composition by adjusting the deposition parameters. The low evaporation temperature deposition avoids oxidation and corrosion of substrates. Chemical deposition results in pin hole free and uniform deposits are easily obtained since ions are more important than the atoms. The film growth can take place by ion-by ion condensation of the materials on the substrates. The preparative parameters can be controlled easily.

In this work, we have synthesized MnTe_2 thin films using CBD method. The influence of pH on the structural and optical properties of MnTe_2 thin films has been investigated in detail. The structural and optical constants of the films are determined from the X-ray diffraction (XRD) and UV-vis spectrophotometric measurements of transmittance, respectively.

2. Experimental details

Firstly, we have prepared telluride solution as follows: 0.02 mol solid crushed tellurium 1-4 dioxan is dissolved inside 0.04 mol potassium hydroxide (KOH). After stirring for 30 min, liquid 1-4 dioxan is separated from the gel by decantation into the another baker. Subsequently, 0.04 mol sodium hydrosulfite (NaHS) is added on the gel telluride when the gel is warmer. We have obtained 100 ml telluride solution (Te_2^{2-} -F) by adding deionized water. The pH of the final telluride solution is measured as approximately 12.70.

Secondly, for obtaining MnTe_2 thin films, 20 ml of 0.01 mol manganese nitrate (MnNO_3)₂ solution is put into the baker. Then, 20 ml telluride solution which is prepared before is added into the same baker and mixed together. The pH of the baths is adjusted as 12, 11, 10 and 9 by adding 2, 4, 6, and 8 ml of 25% HCl solution. Previously cleaned glass substrates (76 mm × 26 mm × 1 mm) are placed vertically to the bottom of the beakers and waited for 24 h at 20 °C. After the deposition, the films are washed with deionized water and dried in air. The reaction of MnTe_2 formation on the glass substrates is as follows:



The crystallographic properties have been investigated by the XRD technique (Bruker AXS D8) using Cu K_α radiation (0.15406 nm). Optical absorption studies are carried out with UV-vis spectrophotometer (Perkin Elmer

Lambda 4S). Film thicknesses are determined by double weight method (i.e. by weighting sample before and after film deposition). Film thicknesses are obtained as 184, 145, 115, and 165 nm for the pH values of the 9, 10, 11, and 12, respectively. As can be seen from Fig. 1, firstly, film thickness decreases from 184 nm to 115 nm with increasing pH value from 9 to 11 and then it increases to the value of 165 nm with increasing pH value of 12.

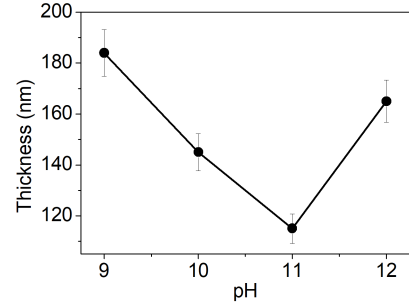


Fig. 1. Dependence of film thickness on pH values with error bars.

3. Results and discussion

Figure 2 shows the XRD patterns of synthesized thin films with various pH values. As can be seen from this figure, the films deposited at pH 9 and 10 are mixture of cubic MnTe_2 (PDF no. 18-813) and orthorhombic MnTe_2O_3 (PDF no. 29-900) structures in Fig. 2a and b, respectively. While the film deposited at pH 11 shows three phases: (1) cubic MnTe_2 , (2) orthorhombic MnTe_2O_3 , and (3) orthorhombic MnTe_2O_5 (PDF no. 30-828) (Fig. 2c). Finally, phases of orthorhombic MnTe_2O_3 and MnTe_2O_5 are found to disappear as the pH of the bath increases to 12, and the film deposited at pH 12 indicates only one phase, cubic MnTe_2 shown in Fig. 2d. This phase also reported by Sharma et al. [21] in which manganese mono and ditelluride thin films were deposited by electrodeposition technique. Comparison of observed and standard 2θ values are listed in Table I. These results show that we have synthesized the best film with cubic structure of MnTe_2 at pH 12.

Figure 3 shows the optical absorbance A , transmittance T and reflectance R spectra of the MnTe_2 films as a function of pH values. It is seen in Fig. 3b that the films indicate a transmittance between 83% and 90% in the visible region, at wavelength of 600 nm.

The optical band gap E_g of the films is determined by the Urbach relation [22]:

$$\alpha = \frac{A(h\nu - E_g)^n}{h\nu}, \quad (1)$$

where α is the absorption coefficient, h is the Planck constant, ν is the frequency of incident photon, A is a constant. The exponent n takes a value of 1/2 for direct allowed transitions, 3/2 direct forbidden transitions, 2.0 for indirect allowed transitions, and 3.0 for indirect forbidden transitions. In Eq. (1), α is evaluated using

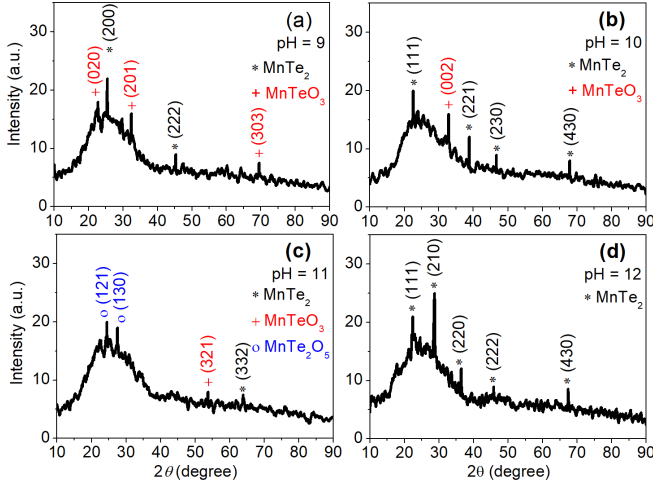


Fig. 2. XRD pattern for the MnTe₂ thin films at different pH values.

TABLE I

Comparison of observed XRD results (2θ [°]) of the MnTe₂ thin films with standard values.

pH	Obs.	Std.	Phase	(hkl)	PDF no.
9	22.857	22.783	orth.	MnTeO ₃ (220)	29-900
	25.229	25.577	cubic	MnTe ₂ (200)	18-813
	29.596	29.063	orth.	MnTeO ₃ (201)	29-900
	45.272	45.092	cubic	MnTe ₂ (222)	18-813
	69.561	69.115	orth.	MnTeO ₃ (303)	29-900
10	22.359	22.150	cubic	MnTe ₂ (111)	18-813
	32.827	32.877	orth.	MnTeO ₃ (002)	29-900
	38.806	38.801	cubic	MnTe ₂ (221)	18-813
	46.648	47.150	cubic	MnTe ₂ (230)	18-813
	67.825	67.307	cubic	MnTe ₂ (430)	18-813
11	24.353	24.921	orth.	MnTe ₂ O ₅ (121)	30-828
	27.464	27.335	orth.	MnTe ₂ O ₅ (130)	30-828
	53.747	53.211	orth.	MnTeO ₃ (321)	29-900
	63.218	62.681	cubic	MnTe ₂ (332)	18-813
12	22.417	22.150	cubic	MnTe ₂ (111)	18-813
	28.719	28.681	cubic	MnTe ₂ (210)	18-813
	36.437	36.557	cubic	MnTe ₂ (220)	18-813
	45.902	45.092	cubic	MnTe ₂ (222)	18-813
	67.447	67.307	cubic	MnTe ₂ (430)	18-813

the relation $\alpha = (1/d) \ln((1-R)^2/T)$, where d is the thickness of the film [23]. The E_g values are obtained by extrapolating the linear portion of the plots of $(\alpha h\nu)^2$ against $h\nu$ to $\alpha = 0$ (Fig. 4). It is seen that E_g value of the films increases from 1.66 eV to 2.62 eV with increasing pH values. These results are higher than the reported data [24], in which manganese mono telluride (MnTe) thin films were deposited by successive ionic layer adsorption and reaction (SILAR) technique, and Ref. [25], in which MnTe thin films were obtained by using electrodeposition method. The corresponding E_g values are also given in Table II.

The refraction index n and extinction coefficient k of MnTe₂ films are given by formulae [26]:

TABLE II

Film thickness and optical parameters of MnTe₂ thin films with various TEA values ($\lambda = 600$ nm).

pH	t [nm]	E_g [eV]	n	k	ε_1	ε_2
9	184	1.66	1.46	0.17	2.11	0.49
10	145	1.73	1.26	0.20	1.54	0.50
11	115	1.83	1.49	0.18	2.18	0.55
12	165	2.62	1.50	0.23	2.20	0.70

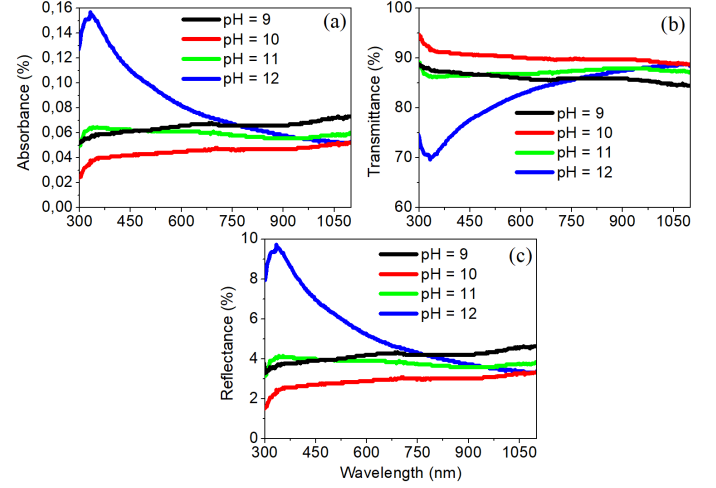


Fig. 3. (a) Absorbance, (b) transmittance and (c) reflectance spectra of MnTe₂ thin films at different pH values.

$$n = \frac{1+R}{1-R} + \sqrt{\frac{4R}{(1-R)^2} - k^2}, \quad (2)$$

$$k = \frac{\alpha\lambda}{4\pi}. \quad (3)$$

The k reflects the absorption of electromagnetic waves in the thin films due to inelastic scattering events. Overall, the n and k values for the films vary inversely with

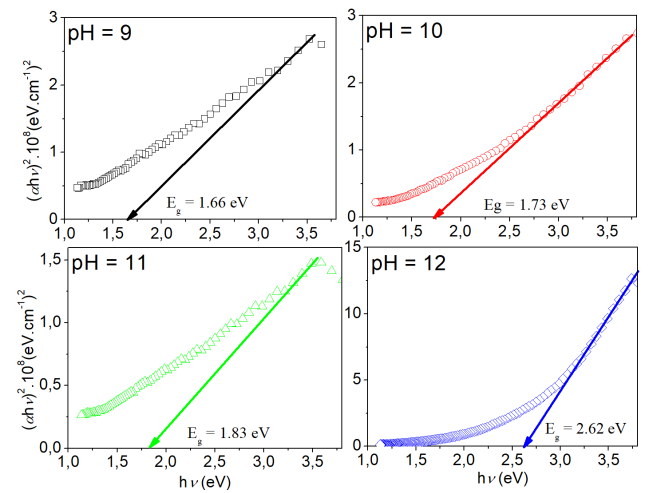


Fig. 4. Plot of $(\alpha h\nu)^2$ versus $h\nu$ for MnTe₂ thin films at various pH values.

transmission. At wavelength of 600 nm, it is clearly seen in Fig. 5a and b that the n and k values change in the range 1.26–1.50 and 0.17–0.23, respectively.

The polarizability of a solid is proportional to its dielectric constant. The real ε_1 and imaginary ε_2 part of the dielectric constants are expressed as follows [27]:

$$\varepsilon_1 = n^2 - k^2, \quad (4)$$

$$\varepsilon_2 = 2nk. \quad (5)$$

Furthermore, the plots of ε_1 and ε_2 are given in Fig. 5c and d, respectively. At wavelength of 600 nm, the ε_1 value varies between 1.54 and 2.20, while the ε_2 value increases from 0.49 to 0.70.

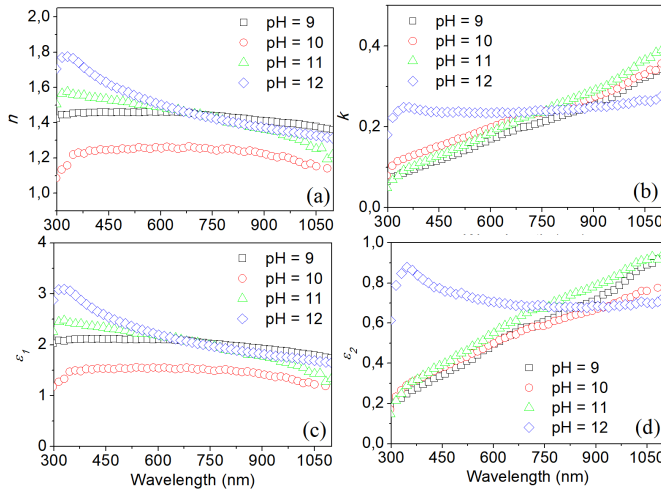


Fig. 5. The variation of (a) refractive index, (b) extinction coefficient, (c) real and (d) imaginary dielectric constant for the MnTe₂ thin films synthesized at different pH values.

4. Conclusion

MnTe₂ thin films are synthesized by CBD method on glass substrates at 20 °C with different pH of the bath. The influence of pH on the crystal structure, and optical properties of the deposited thin films has been investigated in this work. The present films are characterized by using XRD, and UV-vis spectrophotometer. It can be concluded that the pH of the bath affects strongly the formation of MnTe₂ thin films and the best film with good crystallinity and optical properties is synthesized at pH 12 and this film may be more interesting for advanced photovoltaic applications due to its suitable crystal structure and optical properties.

Acknowledgments

This research is fully supported by the Erciyes University Teknopark (Project no. 41).

References

[1] K. Ando, K. Takahashi, T. Okuda, M. Umehara, *Phys. Rev. B* **46**, 12289 (1992).

[2] H. Ohno, *Science* **281**, 951 (1998).
 [3] S. Ünlü, *Phys. At. Nucl.* **75**, 958 (2012).
 [4] N. Ucar, N. Turku, A.F. Ozdemir, A. Calik, *Acta Phys. Pol. A* **130**, 492 (2016).
 [5] W. Laslouni, Z. Hamlati, M. Azzaz, *Acta Phys. Pol. A* **128**, B-190 (2015).
 [6] M. Ustundağ, M. Aslan, *Acta Phys. Pol. A* **130**, 362 (2016).
 [7] O. Boubaker, B. Said, *Acta Phys. Pol. A* **130**, 33 (2016).
 [8] I.H. Karahan, F. Tilti, *Acta Phys. Pol. A* **130**, 282 (2016).
 [9] O. Sahin, S. Uzunoglu E. Sahin, *Acta Phys. Pol. A* **128**, B-145 (2015).
 [10] M. Djamal, Ramli, Khairurrijal, F. Haryanto, *Acta Phys. Pol. A* **128**, B-19 (2015).
 [11] N. Sylva, F. Aliaj, B. Dalipi, *Acta Phys. Pol. A* **130**, 83 (2016).
 [12] E. Karip, S. Aydın, M. Muratoğlu, *Acta Phys. Pol. A* **128**, B-160 (2015).
 [13] A. Tubtimtae, T. Hongto, K. Hongstith, S. Choopun, *Superlatt. Microstruct.* **66**, 96 (2014).
 [14] J. Oleszkiewicz, A. Kisiel, S.A. Ignatowicz, *Thin Solid Films* **157**, 1 (1988).
 [15] A. Martí, G.L. Araújo, *Sol. Energy Mater. Sol. Cells* **43**, 203 (1996).
 [16] F. Göde, E. Güneri, O. Baglayan, *Appl. Surf. Sci.* **318**, 227 (2014).
 [17] G.R. Wu, K. Nagatomo, M. Sasaki, F. Nagasaki, H. Sato, M. Taniguchi, W.X. Gao, *Solid State Commun.* **118**, 425 (2001).
 [18] Z.H. Wang, D.Y. Geng, W.J. Gong, J. Li, Y.B. Li, Z.D. Zhang, *Thin Solid Films* **522**, 175 (2012).
 [19] F. Göde, E. Güneri, F.M. Emen, V.E. Kafadar, S. Ünlü, *J. Lumin.* **147**, 41 (2014).
 [20] A. Kariper, E. Güneri, F. Göde, C. Gümüş, T. Özpozan, *Mater. Chem. Phys.* **129**, 183 (2011).
 [21] R.K. Sharma, G. Singh, Y.G. Shul, H. Kim, *Physica B* **390**, 314 (2007).
 [22] M.G. Sandoval-Paz, M. Sotelo-Lerma, A. Mendoza-Galvan, R. Ramirez-Bon, *Thin Solid Films* **515**, 3356 (2007).
 [23] T.S. Moss, *Optical Properties of Semiconductors*, Academic, New York 1974.
 [24] A. Tubtimtae, K. Arthayakul, B. Teekwang, K. Hongstith, S. Choopun, *J. Coll. Interf. Sci.* **405**, 78 (2013).
 [25] R.K. Sharma, A.C. Rastogi, Gurmeet Singh, *Mater. Chem. Phys.* **84**, 46 (2004).
 [26] N. Benramdane, W.A. Murad, R.H. Misho, M. Ziane, Z. Kebbab, *Mater. Chem. Phys.* **48**, 119 (1997).
 [27] A.K. Wolaton, T.S. Moss, *Proc. Phys. Soc.* **81**, 509 (1963).